Stochastic Models for Local Optical Flow Estimation

Thomas Corpetti and Etienne Mémin

CNRS/LIAMA, Beijing, China & INRIA/FLUMINANCE, Rennes, France
tcorpetti@gmail.com
etienne.memin@inria.fr

Abstract. In this paper, we present a stochastic interpretation of the motion estimation problem. The usual optical flow constraint equation (assuming that the points keep their brightness along time), embed for instance within a Lucas-Kanade estimator, can indeed be seen as the minimization of a stochastic process under some strong constraints. These constraints can be relaxed by imposing a weaker temporal assumption on the luminance function and also in introducing anisotropic intensity-based uncertainty assumptions. The amplitude of these uncertainties are jointly computed with the unknown velocity at each point of the image grid. We propose different versions depending on the various hypothesis assumed for the luminance function. The substitution of our new observation terms on a simple Lucas-Kanade estimator improves significantly the quality of the results. It also enables to extract an uncertainty connected to quality of the motion field.

Keywords: Optical flow, stochastic formulation, brightness consistency assumption.

1 Introduction

Many computer vision problems are formulated on the basis of the spatial and temporal variations of the image luminance:

$$\frac{df}{dt} = \frac{\partial f}{\partial t} + \boldsymbol{v} \cdot \boldsymbol{\nabla} f = 0, \tag{1}$$

where $\boldsymbol{\nabla}$ is the gradient operator in the x and y directions. When the function f denotes the luminance function this equation is referred in Computer Vision as the Optical Flow Constraint Equation (OFCE) or as the brightness consistency assumption and constitutes the only available information for motion estimation issues. Optical flow estimation has been studied intensively since the seminal work of Horn and Schunck [12] and a huge number of methods based on diverse variations of this constraint have been proposed in the literature [5, 9, 20, 22, 23]. Usually a data model constructed from this constraint is associated with some spatial regularizers that promote motion fields with some spatial (and sometimes temporal) coherency. Many authors have proposed on this basis very efficient

A.M. Bruckstein et al. (Eds.): SSVM 2011, LNCS 6667, pp. 701–712, 2012.

techniques. Readers can refer to [4–6, 13, 15–17, 19, 24–26] for a non exhaustive panel or [11] for a recent review. Comparative performance evaluations of some of these techniques can be found in [1, 2, 10]. Among the developed approaches, the techniques focused first on the design of new regularization terms (able for instance to deal with occlusions, discontinuities or relying on physical grounds [8, 11]) and second on the application of advanced minimization strategies. Surprisingly, apart for some specific applications devoted to some specific types of imagery (fluid, biology, infrared imagery, tomography, IRM, ..., see [21] for a summary), only very few authors have worked on generic alternative data terms to the classical brightness consistency assumption, despite the fact it plays a crucial role in the motion estimation process.

The conventional optical flow constraint relation (1) is in fact defined as the differential of a function known only on spatial and temporal discrete point positions (related to the image sequence spatio-temporal lattice). This is somewhat a strong constraint since in practice, the grid points on which is defined the luminance is transported by a flow itself known only up to the same discrete positions. It results from this discretization process an inherent uncertainty on the points location that can reveal to be of important magnitude when are involved strong motions, large inter frames lapse rate or crude spatial discretization associated for instance to large spatial scales measurements. The idea is therefore to encode such a location uncertainty as a random variable and to incorporate the uncertainty transportation into the brightness consistency assumption. This is done using stochastic rules.

The paper is organized as follows: in section 2 we define a stochastic version of the luminance function, by incorporating isotropic and anisotropic uncertainties. From this formulation, two conservation constraints of the image luminance are derived. If the velocity field is available or if we estimate it simultaneously, we propose in section 3 a way to compute the associated uncertainty. Finally, section 4 presents a local multiscale Lucas and Kanade motion estimator based on the brightness consistency stochastic models.

2 Stochastic Luminance Function and Conservation Constraints

2.1 Notations – Conventions

In this paper we use the following conventions/notations:

- the image luminance is f;
- we represent as a vector $\boldsymbol{X} = (\boldsymbol{X}^1, \ldots, \boldsymbol{X}^m)^T$ a grid of $2D$ points, $\boldsymbol{X}^s \in \mathbb{R}^2$;
- the "pixel" grid of the images $\boldsymbol{X}_{t-1}$ is represented by the position of a grid $\boldsymbol{X}$ at the initial time, set to $t-1$
- at time $t-1$, this grid is driven by a velocity field $\boldsymbol{v}(\boldsymbol{X}_{t-1}, t-1) : \mathbb{R}^{2m} \times \mathbb{R}^+ \rightarrow \mathbb{R}^{2m}$ defined on the initial grid $\boldsymbol{X}_{t-1}$ to generate the new point positions $\boldsymbol{X}_t$ at time t.

2.2 Stochastic Luminance Function

We first write the image luminance as the function of a stochastic process related to the position of image points. If one assumes that the velocity $\boldsymbol{v}$ to estimate transports the grid from $\boldsymbol{X}_{t-1}$ to $\boldsymbol{X}_t$ up to a Brownian motion, we can write:

$$d\boldsymbol{X}_t = \boldsymbol{v}(\boldsymbol{X}_{t-1}, t-1)dt + \boldsymbol{\Sigma}(t, \boldsymbol{X}_t)d\mathbf{B}_t, \tag{2}$$

where $\mathbf{B}_t = (\mathbf{B}_t^1, ..., \mathbf{B}_t^m)^T$ is a multidimensional standard Brownian motion of $\mathbb{R}^{2m}$, $\boldsymbol{\Sigma}$ a $(2m \times 2m)$ covariance matrix and $d\boldsymbol{X}_t = \boldsymbol{X}_t - \boldsymbol{X}_{t-1}$ represents the difference between the grid positions. The luminance function f usually defined on spatial points $\boldsymbol{x} = (x, y)$ at time t is here defined on the grid as a map from $\mathbb{R}^+ \times \mathbb{R}^{2m}$ into $\mathbb{R}^m$ and is assumed to be $C^{1,2}(\mathbb{R}^+, \mathbb{R}^{2m})$. Its differential is obtained following the differentiation rules of stochastic calculus (the so called Îto formulae) that gives the expression of the differential of any continuous function of an Îto diffusion of the form in (2) (see [18] for an introduction to stochastic calculus):

$$df(\boldsymbol{X}_t, t) = \frac{\partial f}{\partial t}dt + \sum_{i=(1,2)} \frac{\partial f(\boldsymbol{X}_t, t)}{\partial x_i} dX_t^i + \frac{1}{2} \sum_{(i,j)=(1,2)\times(1,2)} \frac{\partial^2 f(\boldsymbol{X}_t, t)}{\partial x_i \partial x_j} d < X_t^i, X_t^j > . \tag{3}$$

The term $< X_t^i, X_t^j >$ denotes the joint quadratic variations of X^i and X^j and can be computed according to the following rules: $< B^i, B^j >= \delta_{ij} t$ and $< h(t), h(t) >=< h(t), dB^i >=< B^j, h(t) >= 0$ where $\delta_{ij} = 1$ if $i = j$, $\delta_{ij} = 0$ otherwise, and $h(t)$ is a deterministic function. Compared to classical differential calculus, new terms related to the Brownian random terms have been introduced in this stochastic formulation. A possible way to represent the stochastic part of (2) is to use an isotropic uncertainty variance map $\sigma(X_t, t) : \mathbb{R}^+ \times \mathbb{R}^{2m} \rightarrow \mathbb{R}^m$

$$\boldsymbol{\Sigma}(\boldsymbol{X}_t, t)d\mathbf{B}_t = \mathrm{diag}(\sigma(\boldsymbol{X}_t, t)) \otimes \mathbb{I}_2 d\mathbf{B}_t, \tag{4}$$

where $\mathbb{I}_2$ is the (2×2) identity matrix, and $\otimes$ denotes the Kronecker product. Alternatively, one can use anisotropic intensity-based uncertainties along the normal (with a variance σ_η) and the tangent (with a variance σ_τ) of the photometric contour following:

$$\boldsymbol{\Sigma}(\boldsymbol{X}_t, t)d\mathbf{B}_t = \mathrm{diag}(\sigma_\eta(\boldsymbol{X}_t, t)) \otimes \boldsymbol{\eta} dB_t^\eta + \mathrm{diag}(\sigma_\tau(\boldsymbol{X}_t, t)) \otimes \boldsymbol{\tau} dB_t^\tau, \tag{5}$$

where the vectors

$$\boldsymbol{\eta} = \frac{1}{|\boldsymbol{\nabla} f|} \begin{pmatrix} f_x \\ f_y \end{pmatrix}, \boldsymbol{\tau} = \frac{1}{|\boldsymbol{\nabla} f|} \begin{pmatrix} -f_y \\ f_x \end{pmatrix},$$

represent respectively the normal and tangent of the photometric isolines, B^η and B^τ are two scalar independant multidimensional Brownian noises of $\mathbb{R}^m$ and $f_\bullet = \partial f(X_t, t)/\partial \bullet$ for $\bullet = (x, y)$. Let us now express the luminance variations $df(X_t, t)$ under such isotropic or anisotropic uncertainties.

Isotropic Uncertainties. Applying Îto formula (3) to the isotropic uncertainty model yields a luminance variation defined as:

$$df(\boldsymbol{X}_t, t) = \left(\frac{\partial f}{\partial t} + \boldsymbol{\nabla} f \cdot \boldsymbol{v} + \frac{1}{2}\sigma^2 \Delta f \right) dt + \sigma \boldsymbol{\nabla} f \cdot d\boldsymbol{B}_t. \tag{6}$$

Anisotropic Uncertainties. Considering the anisotropic uncertainty model (5) and the mentioned properties regarding the quadratic variations, the term df reads now:

$$df = \left(\frac{\partial f}{\partial t} + \boldsymbol{\nabla} f \cdot \boldsymbol{v} + \frac{\boldsymbol{\nabla} f^T \boldsymbol{\nabla}^2 f \boldsymbol{\nabla} f}{2|\boldsymbol{\nabla} f|^2} (\sigma_\eta^2 - \sigma_\tau^2) + \frac{\sigma_\tau^2 \Delta f}{2} \right) dt + \sigma_\eta \|\boldsymbol{\nabla} f\| dB_t^\eta + \underbrace{\sigma_\tau \boldsymbol{\nabla} f^T \boldsymbol{\tau} dB_t^\tau}_{=0}. \tag{7}$$

In this brightness variation model the stochastic term related to the uncertainty along the tangent vanishes (since the projection of the gradient along the level lines is null). It is straightforward to remark that the standard brightness consistency assumption is obtained from (6) or (7) using zero uncertainties ($\sigma = \sigma_\eta = \sigma_\tau = 0$). The proposed stochastic formulation enables thus to use a softer constraint. From this formulation, let us now derive some generic models for the evolution of the image luminance transported by a velocity field with local uncertainties.

2.3 Uncertainty Models for Luminance Conservation

Starting from a known grid $\boldsymbol{X}_{t-1}$ and its corresponding velocity, the conservation of the image luminance can be quite naturally defined as the conditional expectation $E\left(df(\boldsymbol{X}_t, t) | \boldsymbol{X}_{t-1}\right)$ between $t-1$ and t. To compute this term, we exploit the fact (as shown in appendix A) that the expectation of any function $\Psi(\boldsymbol{X}_t, t)$ of a stochastic process $d\boldsymbol{X}_t$ (as in (2)) knowing the grid $\boldsymbol{X}_{t-1}$ reads:

$$E(\Psi(\boldsymbol{X}_t, t) | \boldsymbol{X}_{t-1}) = \Psi(\boldsymbol{X}_{t-1} + \boldsymbol{v}, t) * \mathcal{N}(0, \boldsymbol{\Sigma}), \tag{8}$$

where $\mathcal{N}(0, \boldsymbol{\Sigma})$ is a multidimensional centered Gaussian. This latter relation indicates that the expectation of a function $\Psi(\boldsymbol{X}_t, t)$ knowing the location $\boldsymbol{X}_{t-1}$ under a Brownian uncertainty of variance $\boldsymbol{\Sigma}$ is obtained by a convolution of $\Psi(\boldsymbol{X}_{t-1} + \boldsymbol{v}, t)$ with a centered Gaussian kernel of variance $\boldsymbol{\Sigma}$.

Assuming $\boldsymbol{\Sigma}$ known, our new conservation model $\mathcal{H}(f, \boldsymbol{v})$ for the luminance evolution is hence defined as (with $g_{\boldsymbol{\Sigma}}$ a gaussian of variance $\boldsymbol{\Sigma}$):

$$\mathcal{H}(f, \boldsymbol{v}) = g_{\boldsymbol{\Sigma}} * (df(\boldsymbol{X}_{t-1} + \boldsymbol{v}, t)) = g_{\boldsymbol{\Sigma}} * \left(\boldsymbol{\nabla} f \cdot \boldsymbol{v} + \frac{\partial f}{\partial t} + \mathcal{F}(f) \right), \text{with} \tag{9}$$

$$\mathcal{F}(f) = \frac{1}{2} \sigma^2 \Delta f \text{ for isotropic uncertainties or } \mathcal{F}(f) = \frac{\boldsymbol{\nabla} f^T \boldsymbol{\nabla}^2 f \boldsymbol{\nabla} f}{2|\boldsymbol{\nabla} f|^2} (\sigma_\eta^2 - \sigma_\tau^2) + \frac{\sigma_\tau^2 \Delta f}{2} \text{ else.} \tag{10}$$

If the brightness conservation constraint strictly holds, one obtains $\sigma = \sigma_\eta = \sigma_\tau = 0$; the Gaussian kernels turn to Dirac distributions and relations (9), (10) correspond to (1). The proposed model provides thus a natural extension of the usual brightness consistency data model. In the next section we propose a way to estimate the uncertainties σ_η and σ_τ.

3 Uncertainty Estimation

Assuming an observed motion field $\boldsymbol{v_{obs}}$ that transports the luminance is available (we will describe in section 5 a local technique for this), it is possible to estimate the uncertainties $\sigma_\eta(\boldsymbol{x}, t)$ and $\sigma_\tau(\boldsymbol{x}, t)$ for each location $\boldsymbol{x}$ at time t.

3.1 Estimation of $\boldsymbol{\sigma_\eta}$

Computing the quadratic variation of the luminance function df between $t-1$ and t yields, for the isotropic or anisotropic version:

$$d\langle f(\boldsymbol{X}_t, t), f(\boldsymbol{X}_t, t)\rangle = \sigma_\eta^2(\boldsymbol{X}_t, t)\|\boldsymbol{\nabla} f(\boldsymbol{X}_t, t))\|^2, \tag{11}$$

where $\sigma = \sigma_\eta$ in the isotropic formulation. This quadratic variation can also be approximated from the luminance f by
$d\langle f(\boldsymbol{X}_t, t), f(\boldsymbol{X}_t, t)\rangle \approx (f(\boldsymbol{X}_t, t) - f(\boldsymbol{X}_{t-1}, t-1))^2$. Considering now that the conditional expectation of both previous terms should be identical, one can estimate the variance by:

$$\sigma_\eta(\boldsymbol{X}_t) = \sqrt{\frac{E\left(f(\boldsymbol{X}_t, t) - f(\boldsymbol{X}_{t-1}, t-1)\right)^2}{E\left(\|\boldsymbol{\nabla} f(\boldsymbol{X}_t, t))\|^2\right)}}. \tag{12}$$

The expectation in the numerator and denominator are then computed at the displaced point $X_{t-1} + \boldsymbol{v_{obs}}(\boldsymbol{X}_{t-1})$ through the convolution of variance $\boldsymbol{\Sigma}(\boldsymbol{X}_{t-1}, t-1)$. A recursive estimation process is thus emerging from equation (12). For the anisotropic model the uncertainty along the tangent is also needed.

3.2 Estimation of $\boldsymbol{\sigma_\tau}$

It is not possible to estimate uncertainty along the tangent of the photometric contours in a similar way since, as shown in (7), this quantity does not appear in the noise associated to the luminance variation and therefore is not involved in the corresponding quadratic variations. Writing the Ito diffusion associated to the velocity projected along the tangent yields

$$\boldsymbol{v_{obs}}^T\boldsymbol{\tau} = \boldsymbol{v}(\boldsymbol{X}_{t-1}, t-1)^T\boldsymbol{\tau}dt + \sigma_\tau(t, \boldsymbol{X}_t)dB_t^\tau. \tag{13}$$

This scalar product constitutes a scalar Gaussian random field of mean $\mu = \boldsymbol{v}(\boldsymbol{X}_{t-1}, t-1)^T\boldsymbol{\tau}$ (assuming $\boldsymbol{v}(\boldsymbol{x}, t)$ is a deterministic function) and covariance $(\mathrm{diag}(\sigma_\tau))$. We assume that the scalar product $\boldsymbol{v}^T\boldsymbol{\tau}$ and the tangent uncertainty $\sigma_\tau(t, \boldsymbol{x})$ are sufficiently smooth in space and can be respectively well approximated by the local empirical mean and variance over a local spatial neighborhood $N(\boldsymbol{x})$ of point $\boldsymbol{x}$:

$$\mu = \frac{1}{|N(\boldsymbol{x})|}\sum_{\boldsymbol{x}_i \in N(\boldsymbol{x})}(\boldsymbol{v_{obs}}(\boldsymbol{x}_i, t-1)^T\boldsymbol{\tau}), \sigma_\tau^2 = \frac{1}{|N(\boldsymbol{x})|-1}\sum_{\boldsymbol{x}_i \in N(\boldsymbol{x})}(\boldsymbol{v_{obs}}(\boldsymbol{x}_i, t-1)^T\boldsymbol{\tau} - \mu)^2. \tag{14}$$

The relations in (9-10) provide new models for the variation of the image luminance under isotropic or anisotropic uncertainties. In this section we have presented a technique to estimate such uncertainties from an available velocity field. The next section focuses on application of those extended brightness consistency models for motion estimation.

4 Application of the Proposed Luminance Models

This section aims at defining a simple local motion estimator that embeds the proposed evolution models as an observation term. As the classical Optical Flow Constraint Equation –OFCE– based on (1), an observation model based on a stochastic evolution of the luminance in (9) is subject to the aperture problem. Similarly to the well-known Lucas-Kanade estimator, we cope this difficulty by assuming constant flow within a Gaussian windowing function of variance σ^ℓ. Therefore, the minimum variance estimate $\boldsymbol{v}$ gives:

$$\left(g_{\sigma^\ell} * g_{\boldsymbol{\Sigma}} * \begin{bmatrix} f_x^2 & f_x f_y \\ f_x f_y & f_y^2 \end{bmatrix}\right) \boldsymbol{v} = -g_{\sigma^\ell} * g_{\boldsymbol{\Sigma}} * (\mathcal{F}(f) + f_t) \begin{bmatrix} f_x \\ f_y \end{bmatrix}. \tag{15}$$

Let us note that in our model the Gaussian windowing function can be interpreted as the distribution of a new isotropic constant uncertainty term related to the grid resolution and independent of the motion uncertainties that do depend on the image data.

A main advantage of such a formulation of the multiresolution setup is to naturally get rid of the use of a pyramidal image representation. With all these elements, we can define the incremental local motion estimation technique:

Incremental Algorithm

1. Initializations :
   - Fix an initial resolution level $\ell = L$
   - Define $\tilde{f}(X_{t-1}, t) := f(X_{t-1}, t)$; $\boldsymbol{v} = 0$;
2. Estimation for the level ℓ
   (a) Initializations :
      - $n = 1$; $\boldsymbol{v}^0 = 0$;
      - Fix a normal uncertainty σ_η^0
      - Fix a tangent uncertainty σ_τ^0 (if anisotropic formulation)
   (b) Estimate σ_η^n by relation (12)
   (c) Estimate σ_τ^n by measuring the tangential uncertainty of $\boldsymbol{v}$ (relation (14))
   (d) Find $\boldsymbol{v}^n$ by local inversions of the system (15)
   (e) Update motion field : $\boldsymbol{v} := \boldsymbol{v} + \boldsymbol{v}^n$
   (f) Warp the image $f(X_t, t)$: $\tilde{f}(X_{t-1}) = f(X_{t-1} + \boldsymbol{v}, t)$
   (g) $n := n + 1$
   (h) **Loop** to step (b) until convergence ($|\boldsymbol{v}^n| < \epsilon$);
3. Decrease the multiresolution level : $\sigma^\ell = \lambda \sigma^\ell$
4. **Loop** to step 2 until convergence ($\sigma^\ell < \sigma^\ell_{min}$).

The previous framework is a natural and simple implementation of a local motion estimation technique using the proposed models for the evolution of the luminance. A quantitative and qualitative evaluation of such an estimator, with comparisons to the classic OFCE will be presented in the next section.

5 Experimental Results

We present in this section some experimental results of the local motion estimator described in section 4. We show examples on synthetic fluid images and

on the Middleburry database[1]. It is important to outline that the estimator defined in section 4 constitutes only a local technique whose aim is only to valid, compare and qualify the observation model based on stochastic uncertainties *vs* the usual ofce in (1). Hence, its performances have to be compared to other local approaches. As a first benchmark we analyze the results obtained on images depicting the evolution of a 2D turbulent fluid flow.

Fluid Images: We used a pair of synthetic images obtained by DNS (Direct Numerical Simulation of Navier-Stokes equations) and representing a 2D turbulent flow. Numerical values of average angular error (AAE) [3] and of the Root Mean Square Error (RMSE) are used as criteria to compare our estimators (isotropic and anisotropic) with some of the state-of-the-art approaches are depicted in table 1. The comparison is done with the following techniques: Horn & Schunck (HS) [12], a commercial software based on correlation (COM, DaVis 7.2 from LaVision GmbH), a pyramidal incremental implementation of the Lucas-Kanade estimator (LK) [14], the proposed framework in section 4 with the OFCE as an observation model (OFCE) (*i.e* with a zero uncertainty), two fluid-dedicated dense motion estimators based on a Div-Curl smoothing with different minimization strategies (DC1–DC2, [8, 27]), a fluid-dedicated dense motion estimator based on a turbulence subgrid model in the data-term (TUR, [7]).

In figure 1, we present an image of the sequence, the estimated flow with the proposed method (anisotropic version) and the error flow field. We have also plotted the velocity spectra of the different techniques and compared them with the ground truth. These spectra are represented in a log-log coordinate and a standard-log coordinate system in order to highlight small and large scales respectively.

On table 1, one can immediately observe that compared to the other local approaches, our method provides very good results since the global accuracy is highly superior than the Lucas-Kanade (LK) and the commercial software (COM). Compared to dense techniques (HS, DC1 and DC2), our numerical results are in the same order of magnitude which is a very relevant point. They are competitive with some dense estimation techniques dedicated to fluid flows analysis with advanced smoothing terms (DC1–DC2, [8, 27]). The comparison between the results OFCE, ISO and ANI is very interesting since it highlights the benefit of the stochastic formulation of the image luminance.

If now one observes the spectra of the velocity we see that the small scales (right part of the graph in fig. 1(g)) are much better recovered by the proposed estimators than by the dense estimators. These latter are generally difficult to estimate and often smoothed out with the spatial regularizers introduced in the dense techniques. Even if the Lucas-Kanade technique seems to exhibit better results on small scales, when observing the figure 1(h), it is obvious to note that large scales are badly estimated with this approach and this yields a very poor overall accuracy (see table 1). As for the large scales the results are comparable

[1] `http://vision.middlebury.edu/flow/`

with the best dense dedicated techniques. We believe hence that our estimator constitutes an appealing alternative to usual local PIV methods. Let us now describe the accuracy of the observation term on some images of the middleburry database.

Table 1. Quantitative comparisons on the DNS sequence

	LK	COM	HS	DC 1	DC 2	TUR	OFCE	ISO	ANISO
AAE	6.07^o	4.58^o	4.27^o	4.35^o	3.04^o	4.49^o	4.53^o	3.59^o	3.12^o
RMSE	0.1699	0.1520	0.1385	0.1340	0.09602	0.1490	0.1243	0.1072	0.0961

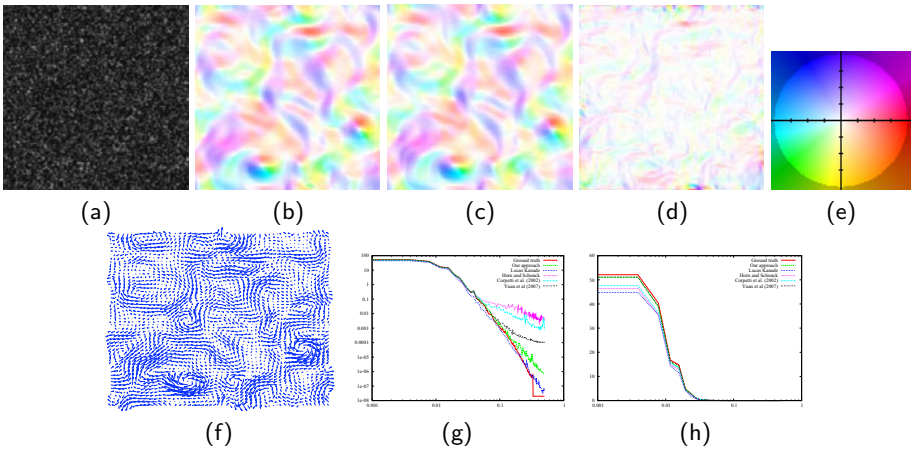

Fig. 1. Results on the DNS sequence : Top (a): an image of the sequence; (b): the estimated flow ; (c): the real flow; (d): the difference flow represented with the coding color in (e); **Bottom** (f): visualisation of the estimated flow; (g-h): Spectra of the velocity compared with ground truth and to several method: (g): log-log representation (highlights small scales on the right part) and (h): non log-log representation (highlights large scales on the left part). Color are : Red : ground truth; Green : our approach (anisotropic version); Blue : Lucas-Kanade [14]; Purple : Horn and Schunck [12]; Cyan: Div-Curl smoothing [8] and Black: Div-Curl in mimetic discretization [27]

Middleburry Database: We have tested our approaches on the "Dimetrodon", "Yosemite" and "Venus" sequences. For these sequences ground truths comparisons with others state-of-the-art approaches are available. The dimetrodon sequence is illustrated in figure 2.

The quantitative results are presented in the table 2. When comparing the three first columns that use exactly the same technique but based on the usual OFCE (relation (1)), our luminance model with isotropic (ISO) and anisotropic (ANISO) uncertainties (relation (10)), it immediately points out that the proposed models enable to enhance significantly the quality of the results. This fair

comparison of the three observation models onto the same estimator promotes the use of a stochastic formulation under anisotropic uncertainties. In fact this latter version is a softer constraint than the OFCE which, as shown previously, assumes implicitly a perfect measurement without any incertitudes. The estimated motion fields under the anisotropic luminance formulation is represented on figure fig.2 (c) and can be compared with the ground truth in fig.2(d).

Let us in addition remind that the motion estimation technique that has been developed for comparing the models of luminance is quite simple (based on Lucas and Kanade). Therefore, as expected, the errors are mainly localized on discontinuities. However it is very informative to observe that despite the simplicity of this technique, our results in table 2 are very competitive and sometimes outperform advanced dense techniques with a specific process for discontinuities. Apart from regions exhibiting motion discontinuities and where the error can be important, the difference fields of fig.2(d) reveals very good results (white areas) in the other locations. This suggests that the luminance models introduced in this paper is usefull in allowing a global improvement of accuracy. More than the estimated motion fields, such a technique is able to extract the associated uncertainty areas. The norm of the global uncertainty $\sqrt{\sigma_\eta^2 + \sigma_\tau^2}$ map obtained at the end of the process with the best estimator (the anisotropic one) is plotted in fig.2(e). As expected, homogeneous areas where the aperture problem holds correspond to high values whereas small values are linked to photometric contours. Such output of our method is very promising since it it highlights the main structures of the images and gives an indicator of the quality of the estimation. To justify this last point, we have depicted in fig.2(f) the reconstructed errors when we take into account for the evaluation only the points where the incertitude is bellow a given value (blue lines) and the corresponding percentage of points used for the computation (red lines).

We then strongly believe that the stochastic models presented can be exploited in the future to design dense estimators relying on the proposed brightness consistency model.

Table 2. Quantitative results and comparisons on the Dimetrodon, Yosemite and Venus sequence

Results on the Dimetrodon sequence

Met.	OFCE	ISO	ANISO	Bruhn et al.	Black, Ana.	Pyr. LK	Med. Pla.^{TM}	Zitnick et al
Ang. err.	7.95^o	3.95^o	$\mathbf{2.85}^o$	10.99^o	9.26^o	10.27^o	15.82^o	30.10^o

Results on the Yosemite sequence

Met.	OFCE	ISO	ANISO	Bruhn et al.	Black, Ana.	Pyr. LK	Med. Pla.^{TM}	Zitnick et al
Ang. error	4.47^o	3.12^o	2.89^o	$\mathbf{1.69}^o$	2.65^o	5.22^o	11.09^o	18.50^o

Results on the Venus sequence

Met.	OFCE	ISO	ANISO	Bruhn et al.	Black, Ana.	Pyr. LK	Med. Pla.^{TM}	Zitnick et al
Ang. error	12.02^o	10.23^o	8.42^o	8.73^o	$\mathbf{7.64}^o$	14.61^o	15.48^o	11.42^o

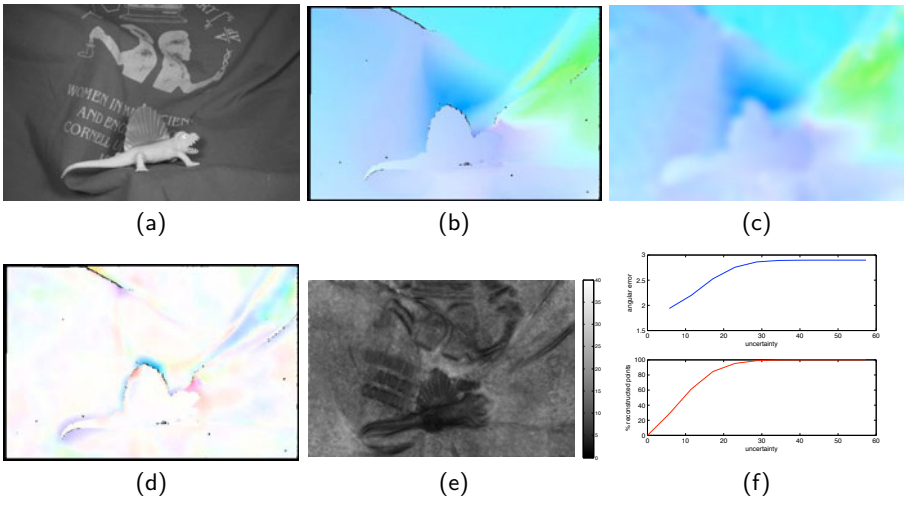

Fig. 2. Dimetrodon sequence (a): an image of the sequence; (b): the ground truth; (c): The estimated motion field with our approach in anisotropic version; (d): difference velocity field and (e): the extracted uncertainty map σ_η and (f): evolution of the error and percentage of correct motion fields when one takes into account only velocity fields with smaller values of $\sqrt{\sigma_\eta^2 + \sigma_\tau^2}$

6 Conclusion

In this paper an observation model for optical flow estimation has been introduced. The new operator is based on a stochastic modeling of the brightness consistency uncertainty. This data model constitutes a natural extension of the usual brightness consistency assumption. Isotropic and anisotropic uncertainty models have been presented. From this new data term, we have designed a simple local motion estimator where the multiresolution is also interpreted in term of a spatial uncertainty.

The performances of this local estimator have been validated on synthetic fluid flows issued from Direct Numerical Simulations and on the middleburry synthetic database. In the first case, the results have exhibited significant performances, especially in the recovery of small scales that are generally smoothed out by spatial regularizers of dense approaches. As for the middleburry database, the simple local implementation of the presented data-term outperforms local approaches. We therefore believe that this stochastic modeling is a very promising alternative to the usual deterministic OFCE for all optical-flow methods.

A Expectation of a Function of a Stochastic Process

The conditional expectation given $\boldsymbol{X}_{t-1}$ of any function $\Psi(\boldsymbol{X}_t, t)$ of a stochastic process defined through Îto diffusion (3) and discretized through an Euler scheme $\boldsymbol{X}_t = \boldsymbol{X}_{t-1} + \boldsymbol{v}(\boldsymbol{X}_{t-1})dt + \boldsymbol{\Sigma}^{1/2}(B_{t+1} - B_t)$ may be written as:

$$E(\Psi(\boldsymbol{X}_t,t)|\boldsymbol{X}_{t-1}) = \int_{\mathbb{R}} \Psi(\boldsymbol{X}_t,t)p(\boldsymbol{X}_t|\boldsymbol{X}_{t-1})d\boldsymbol{X}_t. \tag{16}$$

As the process $\boldsymbol{X}_t$ is known up to the Brownian motion $\boldsymbol{\Sigma}d\boldsymbol{B}_t$, the probability $p(\boldsymbol{X}_t|\boldsymbol{X}_{t-1})$ is a multidimensional Gaussian of variance $\boldsymbol{\Sigma}\sqrt{dt}$ ($dt = 1$ here) and we get:

$$E(\Psi(\boldsymbol{X}_t)|\boldsymbol{X}_{t-1}) = \frac{1}{\sqrt{2\pi}\det(\boldsymbol{\Sigma})^{\frac{1}{2}}} \int_{\mathbb{R}} \Psi(\boldsymbol{X}_t,t) \exp\left(-(\boldsymbol{X}_{t-1}+\boldsymbol{v}-\boldsymbol{X}_t)\boldsymbol{\Sigma}^{-1}(\boldsymbol{X}_{t-1}+\boldsymbol{v}-\boldsymbol{X}_t)\right) d\boldsymbol{X}_t. \tag{17}$$

By a change of variable $\mathbf{Y}_t = \boldsymbol{X}_{t-1} + \boldsymbol{v} - \boldsymbol{X}_t$, this expectation can be written as:

$$\begin{aligned} E(\Psi(\boldsymbol{X}_t,t)|\boldsymbol{X}_{t-1}) &= \frac{1}{\sqrt{2\pi}\det(\boldsymbol{\Sigma})^{1/2}} \int_{\mathbb{R}} \Psi(\boldsymbol{X}_{t-1}+\boldsymbol{v}-\mathbf{Y}_t,t)\exp\left(-\mathbf{Y}_t\boldsymbol{\Sigma}^{-1}\mathbf{Y}_t\right)d\mathbf{Y}_t \\ &= \Psi(\boldsymbol{X}_{t-1}+\boldsymbol{v},t) * \mathcal{N}(0,\boldsymbol{\Sigma}). \end{aligned} \tag{18}$$

References

1. Baker, S., Scharstein, D., Lewis, J., Roth, S., Black, M., Szeliski, R.: A database and evaluation methodology for optical flow. In: Int. Conf. on Comp. Vis. (2007)
2. Barron, J., Fleet, D., Beauchemin, S.: Performance of optical flow techniques. Int. J. Comput. Vis. 12(1), 43–77 (1994)
3. Barron, J.L., Fleet, D.J., Beauchemin, S.S., Burkitt, T.A.: Performance of optical flow techniques. Int. J. of Comp. Vis. 12(1), 43–77 (1994)
4. Black, M., Anandan, P.: Robust incremental optical flow. In: Eklundh, J.-O. (ed.) ECCV 1994. LNCS, vol. 800, pp. 296–302. Springer, Heidelberg (1994)
5. Brox, T., Bruhn, A., Papenberg, N., Weickert, J.: High accuracy optical flow estimation based on a theory for warping. In: Pajdla, T., Matas, J(G.) (eds.) ECCV 2004. LNCS, vol. 3024, pp. 25–36. Springer, Heidelberg (2004)
6. Bruhn, A., Weickert, J., Kohlberger, T., Schnoerr, C.: A multigrid platform for real-time motion computation with discontinuity-preserving variational methods. Int. J. Com. Vis. 70(3), 257–277 (2006)
7. Cassisa, C., Simoens, S., Prinet, V.: Two-frame optical flow formulation in an unwarping multiresolution scheme. In: Bayro-Corrochano, E., Eklundh, J.-O. (eds.) CIARP 2009. LNCS, vol. 5856, pp. 790–797. Springer, Heidelberg (2009)
8. Corpetti, T., Mémin, E., Pérez, P.: Dense estimation of fluid flows. IEEE Trans. Pattern Anal. Machine Intell. 24(3), 365–380 (2002)
9. Fitzpatrick, J.: The existence of geometrical density-image transformations corresponding to object motion. Com. Vis., Grap., Im. Proc. 44(2), 155–174 (1988)
10. Galvin, B., McCane, B., Novins, K., Mason, D., Mills, S.: Recovering motion fields: an analysis of eight optical flow algorithms. In: Proc. British Mach. Vis. Conf., Southampton (1998)
11. Heitz, D., Mémin, E., Schnoerr, C.: Variational fluid flow measurements from image sequences: synopsis and perspectives. Exp. Fluids 48(3), 369–393 (2010)
12. Horn, B., Schunck, B.: Determining optical flow. Artificial Intelligence 17, 185–203 (1981)
13. Lempitsky, V., Roth, S., Rother, C.: Fusionflow: Discrete-continuous optimization for optical flow estimation. In: IEEE Comp. Vis. Patt. Rec. (2008)

14. Lucas, B., Kanade, T.: An iterative image registration technique with an application to stereovision. In: Int. Joint Conf. on Art. Int., pp. 674–679 (1981)
15. Mémin, E., Pérez, P.: Dense estimation and object-based segmentation of the optical flow with robust techniques. IEEE Trans. Im. Proc. 7(5), 703–719 (1998)
16. Nagel, H.: Extending the oriented smoothness constraint into the temporal domain and the estimation of derivatives of optical flow. In: Faugeras, O. (ed.) ECCV 1990. LNCS, vol. 427, pp. 139–148. Springer, Heidelberg (1990)
17. Nesi, P.: Variational approach to optical flow estimation managing discontinuities. Image and Vision Computing 11(7), 419–439 (1993)
18. Oksendal, B.: Stochastic differential equations. Spinger, Heidelberg (1998)
19. Papenberg, N., Bruhn, A., Brox, T., Didas, S., Weickert, J.: Highly accurate optic flow computation with theoretically justified warping. Int. J. Comput. Vision 67(2), 141–158 (2006)
20. Schunck, B.: The image flow constraint equation. Com. Vis., Grap., Im. Proc. 35, 20–46 (1986)
21. Sun, D., Roth, S., Black, M.: Secrets of optical flow estimation and their principles. In: Proc. IEEE Com. Vis. and Pat. Rec., CVPR 2010, pp. 2432–2439 (2010)
22. Tretiak, O., Pastor, L.: Velocity estimation from image sequences with second order differential operators. In: Proc. 7th Int. Conf. On Pattern Recognition, Montreal, pp. 16–19 (1984)
23. Weber, J., Malik, J.: Robust computation of optical flow in a multi-scale differential framework. Int. J. Comput. Vis. 14(1) (1995)
24. Wedel, A., Pock, T., Braun, J., Franke, U., Cremers, D.: Duality tv-l1 flow with fundamental matrix prior. In: Image Vision and Computing, Auckland, New Zealand (November 2008)
25. Weickert, J., Schnörr, C.: Variational optic-flow computation with a spatio-temporal smoothness constraint. J. Math. Im. and Vis. 14(3), 245–255 (2001)
26. Xu, L., Chen, J., Jia, J.: A segmentation based variational model for accurate optical flow estimation. In: Forsyth, D., Torr, P., Zisserman, A. (eds.) ECCV 2008, Part I. LNCS, vol. 5302, pp. 671–684. Springer, Heidelberg (2008)
27. Yuan, J., Schnörr, C., Mémin, E.: Discrete orthogonal decomposition and variational fluid flow estimation. Journ. of Mathematical Imaging and Vision 28(1), 67–80 (2007)